

# Mass Balance Modeling of Vanillin Production from Vanillic Acid by Cultures of the Fungus *Pycnoporus cinnabarinus* in Bioreactors

Olivier Bernard,<sup>1</sup> Georges Bastin,<sup>2</sup> Christelle Stentelaire,<sup>3</sup>  
Laurence Lesage-Meessen,<sup>3</sup> Marcel Asther<sup>3</sup>

<sup>1</sup>Comore, Inria, BP 93, 06902 Sophia-Antipolis Cedex, France

<sup>2</sup>Cesame, Université Catholique de Louvain, Avenue G. Lemaitre, 4-6, 1348 Louvain-La-Neuve, Belgium; telephone: +32 10 47 80 38; fax: +32 10 47 21 80; e-mail: bastin@csam.ucl.ac.be

<sup>3</sup>Laboratoire de Biotechnologie des Champignons Filamenteux, INRA, CESB-ESIL, 163 Avenue de Luminy, Case Postale 925, 13288 Marseille Cedex 09, France

Received 10 June 1998; accepted 10 June 1999

**Abstract:** A systematic two-step procedure for the structural identification of bioprocesses is followed in order to establish a mechanistic model for vanillin production by *Pycnoporus cinnabarinus*. The first step is devoted to the identification of the underlying reaction structure and the development of a validated mass balance model for the growth of *P. cinnabarinus* and the biotransformation of vanillic acid into vanillin. The second step is devoted to the kinetic modeling, namely, the estimation of the reaction rates and the calibration of the kinetic parameters. The whole procedure leads to the final set up of a simulation model of the process. The results are supported by the data from five cultures of *P. cinnabarinus* in bioreactors. © 1999 John Wiley & Sons, Inc. *Biotechnol Bioeng* 65: 558–571, 1999.

**Keywords:** bioprocess modeling; filamentous fungi; *Pycnoporus cinnabarinus*; vanillic acid; vanillin; mass balance model

## INTRODUCTION

Recently, the increasing interest in natural products led to develop flavor production via biotechnological processes involving microorganisms. An important attribute of microbial biocatalysts in bioreactors is the ability to synthesize products in a consistent and predictable manner. The aim of this paper is to present a mechanistic model for the production in bioreactor of vanillin, the most universally used flavor in the food industry, by the fungus *Pycnoporus cinnabarinus*. Vanillic acid, an intermediate in the degradation of lignin by white-rot fungi, has been reported to be a suitable substrate for vanillin production (Falconnier et al., 1994; Lesage-Meessen et al., 1996). The model is intended to be

used for the development of model-based monitoring and optimal process control strategies.

The model is set up by a systematic and rigorous application of a general two-step procedure for the structural identification of bioprocesses (Bastin et al., 1997). The first step is devoted to the identification of the underlying reaction structure and the development of a validated mass balance model for the growth of *P. cinnabarinus* and the biotransformation of vanillic acid into vanillin. The identification of the yield coefficients, the estimation of mortality during the production phase, and the sugar utilization for vanillin production are successively considered. The second step is devoted to the kinetic modeling, namely, the estimation of the reaction rates and the calibration of the kinetic parameters. The model identification task is supported by six fed-batch cultures in a pilot bioreactor: one control culture of *P. cinnabarinus* and five production cultures to which pure chemical vanillic acid is added as a precursor of vanillin biosynthesis after a mycelium-producing phase. Finally, the methodology leads to the final setup of a “control design oriented” simulation model of the process.

Similar models have been previously published in the literature for other filamentous fungi, e.g. *Penicillium* sp. (Bajpai and Reuss, 1981; Suijdam et al., 1982) or *Aspergillus* sp. (Torres, 1994). To our knowledge, the model presented in the present paper is the first one published concerning the biotransformation of vanillic acid to vanillin using basidiomycetes.

More complicated structured modeling approaches relying on a detailed description of the fungal growth by elongation and branching have also been considered in the literature (see e.g. Nestaas and Wang, 1983; Aynsley, et al., 1990; Paul and Thomas, 1996). However, such an approach is not followed here because it leads to mathematical models that are less convenient to be used for monitoring and control design.

Correspondence to: G. Bastin

Contract grant sponsor: European Research Programme

Contract grant number: ERB-FAIR-CT96-1099

## MATERIAL AND METHODS

### Fungal Strain

The strain used in this study was *P. cinnabarinus* MUCL 39533, a monokaryotic laccase-deficient strain obtained from the Mycothèque de l'Université Catholique de Louvain (Louvain-La-Neuve, Belgique). The strain was maintained on a malt agar slant.

### Medium and Culture Conditions

Fungal cultures were grown in a basal medium previously described (Gross-Falconnier, 1994). This medium contained maltose as carbon source (20 g L<sup>-1</sup>), diammonium tartrate (1.842 g L<sup>-1</sup>) as nitrogen source, yeast extract (0.5 g L<sup>-1</sup>), KH<sub>2</sub>PO<sub>4</sub> (0.2 g L<sup>-1</sup>), CaCl<sub>2</sub> (0.0132 g L<sup>-1</sup>), and MgSO<sub>4</sub> (0.5 g L<sup>-1</sup>). The liquid preculture was prepared as follows: mycelium was grown for 10 days on a medium with 2.5 g L<sup>-1</sup> cellobiose as the carbon source and then collected and mixed with sterile water using an Ultra-Turrax T25 blender (Janke & Kunkel, GmbH & Co. KG, Staufen, Germany). A 200-mL amount of this suspension was inoculated into the bioreactor containing 1.6 L of basal medium. The cultures were realized in 2-L bioreactor of a standard geometry, mechanically agitated with a marine propeller. Agitation rate was 120 rpm for the first 3 days to prevent the adhesion of the mycelia to the propeller, and was then shifted to 100 rpm until the end of the fermentation. Air was injected through a perforated pipe sparger. The core temperature was held at 30°C. The bioreactor was connected to a computer via a process interface to measure on-line pH and dissolved oxygen.

The experimental conditions are given in Table I. Experiment A is a pure culture of *P. cinnabarinus* while in experiments B, C, D, E, and F an initial batch growth phase of 3 days is followed by a fed-batch production phase with continuous addition of pure chemical vanillic acid (used as filtered salt solution) to the culture medium. Cellobiose (2.5 g L<sup>-1</sup>) was added to the culture medium 2 h before the continuous addition of vanillic acid (Lesage-Meessen et al., 1997).

These experimental conditions have been chosen to have a significant vanillin production (about 1.2 g L<sup>-1</sup> at the end of the fermentation). As it can be seen in Table I the various experiments differ mainly in the aeration rates with a view to characterizing the oxygen influence on the vanillin production.

As a matter of illustration, an excerpt of the measurements collected during experiments C and D is shown in Fig. 1 (the whole set of data is presented in the sequel with the simulation results (Figs. 9 and 10)). It is worth noting that the growth stops very soon after the feeding of vanillic acid.

### Fungal Biomass Measurement

Dry weight of the mycelium was measured after filtration on GF/A glass-fiber filters (Whatman, Maidstone, England) and drying overnight at 105°C.

### Measurement of Phenolic Metabolites

Samples were filtered through 0.2- $\mu$ m syringe filters (Microgrog Inc, DynaGard, Laguna Hills, CA) and analyzed from days 4 to 8 by HPLC (25  $\mu$ L injected). An HPLC Model 1050 (Hewlett-Packard, Rockville, MD), equipped with a variable UV/vis detector set at 280 nm and a 34-position autosampler–autoinjector, was used. The mobile phase, at a flow rate of 1 mL min<sup>-1</sup>, comprised a mixture of two degassed solvents: A, 0.01% acetic acid in water and B, methanol. The elution was performed with solvent B starting at 20% held for 4 min, then increased to 40% during 24 min, and then increased after 27 min to 100% at which it was held for a further 2 min. Solvent B was reduced to 20% after 30 min and the column was re-equilibrated for at least 5 min before the next injection. Quantification was performed using external standards.

### Carbon Determination

Isocratic HPLC analysis on an ion-exchange column maintained at 80°C (Bio-Rad, Richmond, CA, Aminex ion-exclusion HPX-87P, 300  $\times$  7.8 mm) using a Model 1050

**Table I.** Experimental conditions of the six considered experiments.

Exp.	Batch mycelium producing phase		Fed-batch vanillin producing phase			
	Duration (days)	Air flow rate (l/h)	Feed flow rate (ml/day)		Feeding vanillic acid $A_m$ (mol/l)	Air flow rate (l/h)
			Days 4–5	Days 6–7		
A	8	30	—	—	—	—
B	3	30	27	27	0.238	30
C	3	60	27	18	0.238	30
D	3	60	27	18	0.238	40
E	3	60	27	18	0.238	20
F	3	90	27	18	0.238	30

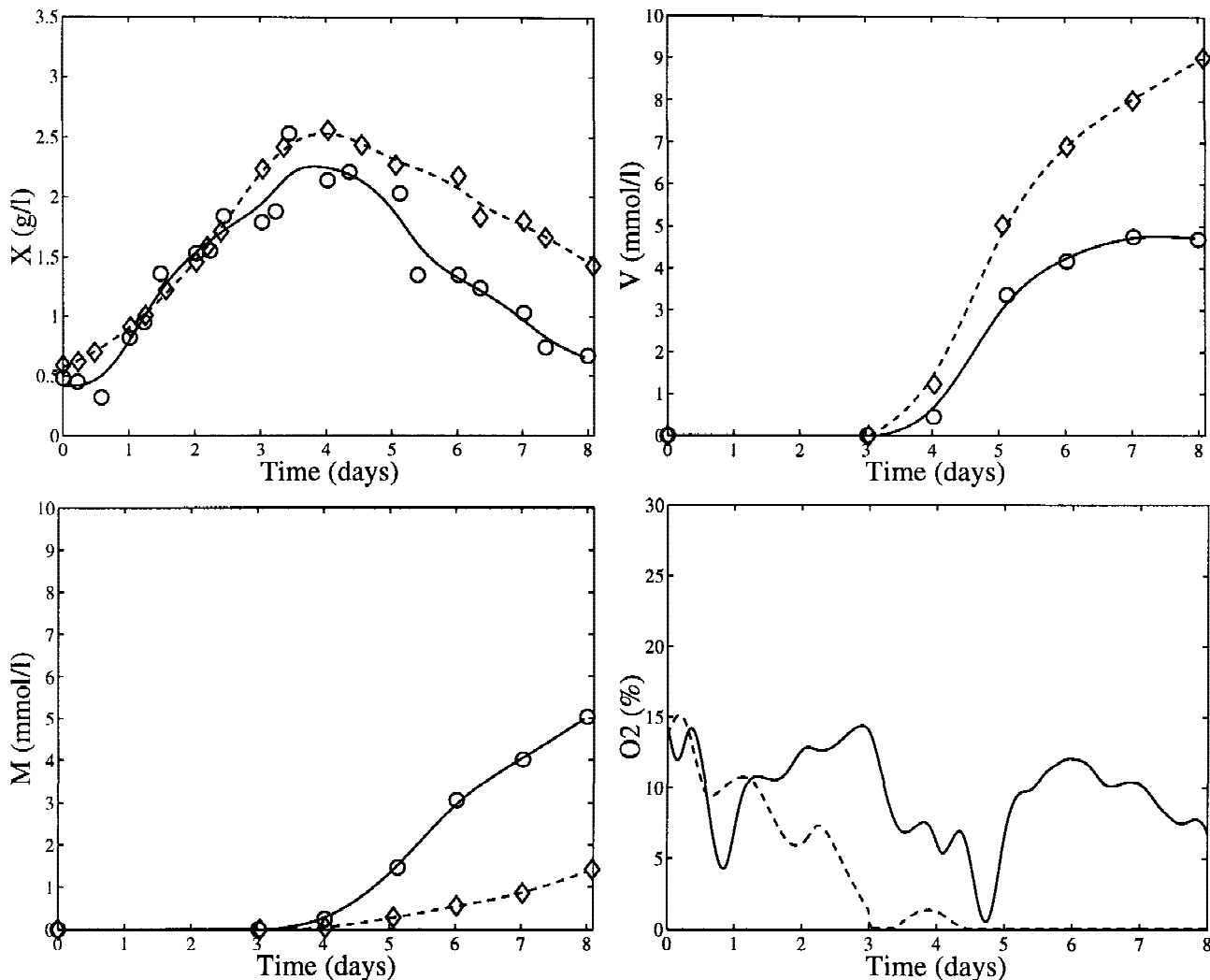


**Figure 1.** Measurements of biomass ( $X$ ), vanillin ( $V$ ), methoxyhydroquinone ( $M$ ), and oxygen ( $O$ ) for experiments C ( $\diamond$ ) and D ( $\circ$ ). The continuous lines are the smoothing splines that will be used in the sequel (C, --; D, —).

HPLC (Hewlett-Packard, Rockville, MD) equipped with a refractive index detector and a 34-position autosampler–autoinjector, was carried out directly on culture filtrates for the maltose, cellobiose, and glucose determination. The eluent was water at a flow rate of  $0.4 \text{ mL}\cdot\text{min}^{-1}$ . A chromatograph was connected to the HP 3365 Chem Station for chromatographic data processing and quantification was performed using external standards. Maltose, glucose, and cellobiose were determined and quantified.

### Ammonium Determination

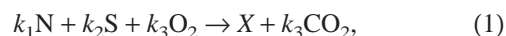
Ammonium was measured quantitatively using the Spectroquant 14752 Ammonium Method (Merck, Darmstadt, Germany). In alkaline medium, ammonium reacted with hypochloride and thymol to form blue indophenol. The reaction was monitored at 690 nm. Ammonium chloride was used as the standard.

## RESULTS AND DISCUSSION

### Mass Balance Modeling

The objective is to progressively derive a mass balance model which is based on a set of biological reactions and is able to describe the behaviour of the process, namely the growth of *P. cinnabarinus* and the biotransformation of vanillic acid into vanillin in bioreactors.

The aerobic growth of the fungal biomass ( $X$ ) from a carbon source ( $S$ ) and a nitrogen source ( $N$ ) is represented by the following reaction



where the coefficients  $k_1$ ,  $k_2$ , and  $k_3$  represent the yield coefficients associated to nitrogen consumption, sugar consumption, and oxygen respiration, respectively. As mentioned previously, the carbon source is made up of sugars

(glucose and maltose considered together as a single species), and the nitrogen source is ammonium.

The yield coefficients  $k_1$  and  $k_2$  will be estimated in the next section, and two biomass estimators will be derived on the basis of data collected when the growth proceeds without biotransformation (Expt. A and the first 3 days of Expts. B and C).

Afterward, the second phase of Expts. B and C (with simultaneous growth and biotransformation) will be used to evaluate the mortality and the sugar consumption needed for the secondary metabolism. Finally, the mass balance model will be used to compute estimates of the time evolution of the reaction rates.

### Estimation of $k_1$ and $k_2$

When the growth takes place in a stirred tank bioreactor, the mass balance equations corresponding to reaction (1) are written as

$$\frac{dX}{dt} = r_1 - DX, \quad (2)$$

$$\frac{dN}{dt} = -k_1 r_1 - DN + DN_{in}, \quad (3)$$

$$\frac{dS}{dt} = -k_2 r_1 - DS + DS_{in}, \quad (4)$$

where  $X$ ,  $N$ ,  $S$  denote biomass, nitrogen and sugar concentrations, respectively.  $N_{in}$  and  $S_{in}$  are the nitrogen and sugar concentrations in the feeding medium respectively.  $r_1$  denotes the fungal growth rate and the dilution rate  $D$  is the ratio of the influent flow rate  $F$  over the volume of the bioreactor (obviously  $D = 0$  for batch cultures).

By eliminating the reaction rate  $r_1$  between Eqs. (2) and (3) and (2) and (4), respectively, the following relations are obtained:

$$\frac{d}{dt} [k_1 X + N] = -D(k_1 X + N) + DN_{in}, \quad (5)$$

$$\frac{d}{dt} [k_2 X + S] = -D(k_2 X + S) + DS_{in}. \quad (6)$$

These equations are then integrated between time instants 0 and  $t$ :

$$k_1 \left[ X(t) + \int_0^t D(\tau) X(\tau) d\tau \right] + \left[ N(t) + \int_0^t D(\tau) N(\tau) d\tau \right] - \left[ k_1 X(0) + N(0) + N_{in} \int_0^t D(\tau) d\tau \right] = 0, \quad (7)$$

$$k_2 \left[ X(t) + \int_0^t D(\tau) X(\tau) d\tau \right] + \left[ S(t) + \int_0^t D(\tau) S(\tau) d\tau \right] - \left[ k_2 X(0) + S(0) + S_{in} \int_0^t D(\tau) d\tau \right] = 0. \quad (8)$$

To simplify the notations, we introduce the function  $\phi$  computed from any function of time  $y(t)$  as follows:

$$\phi[y(t)] = y(t) + \int_0^t D(\tau) y(\tau) d\tau. \quad (9)$$

Using this compact notation, Eqs. (7) and (8) become

$$k_1 \phi[X(t)] + \phi[N(t) - N_{in}] - (k_1 X(0) + N(0) - N_{in}) = 0, \quad (10)$$

$$k_2 \phi[X(t)] + \phi[S(t) - S_{in}] - (k_2 X(0) + S(0) - S_{in}) = 0. \quad (11)$$

These linear relationships can be used to estimate the parameters  $k_1$  and  $k_2$  with a simple linear regression. To compute the regression, the data of  $X(t)$ ,  $N(t)$ , and  $S(t)$  are interpolated and smoothed using cubic splines (MATLAB Toolbox). The splines are then integrated numerically in order to compute approximations of the integrals at the interpolation instants.

Three experiments have been used for this linear regression: an experiment with pure fungal growth (Expt. A), and the biomass growth phase of two other experiments with biotransformation (Expts. B and C).

The following parameter estimates are obtained:

$$\hat{k}_1 = 4.7 \text{ mmol g}^{-1}, \quad \hat{k}_2 = 4.9 \text{ g g}^{-1}. \quad (12)$$

### Biomass Estimators

Eqs. (5) and (6) are first-order linear differential equations that can be integrated analytically. The solution is written as follows:

$$k_1 X(t) + N(t) = [k_1 X(0) + N(0) - N_{in}] \exp\left(-\int_0^t D(\tau) d\tau\right) + N_{in}, \quad (13)$$

$$k_2 X(t) + S(t) = [k_2 X(0) + S(0) - S_{in}] \exp\left(-\int_0^t D(\tau) d\tau\right) + S_{in}. \quad (14)$$

From the measurements of  $N$  or  $S$ , the two following biomass estimators ( $\hat{X}_1(t)$  and  $\hat{X}_2(t)$ ) can be derived from Eqs. (13) and (14) once estimates of  $\hat{k}_1$  and  $\hat{k}_2$  are available.

$$\hat{X}_1(t) = \left[ X(0) + \frac{N(0) - N_{in}}{\hat{k}_1} \right] \exp\left(-\int_0^t D(\tau) d\tau\right) + \frac{N_{in} - N(t)}{\hat{k}_1}, \quad (15)$$

$$\hat{X}_2(t) = \left[ X(0) + \frac{S(0) - S_{in}}{\hat{k}_2} \right] \exp\left(-\int_0^t D(\tau) d\tau\right) + \frac{S_{in} - S(t)}{\hat{k}_2}. \quad (16)$$

Note that the inoculum  $X(0)$  must be known to compute the estimations. However, it can be proved that  $\hat{X}_1$  and  $\hat{X}_2$  are asymptotic estimators of the biomass  $X$ , since the error

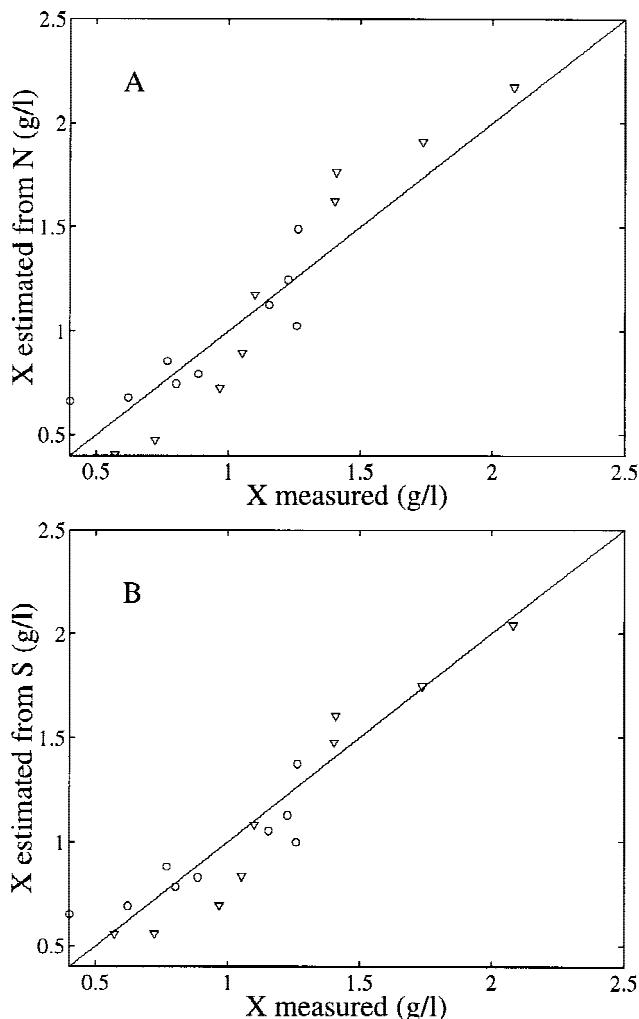


**Figure 2.** Cross-validation of Eqs. (15) and (16) with experiments E and F. The figure presents the comparison of the measured biomass  $X$  and of the estimates  $\hat{X}$  computed: (A) from measurements of  $N$  (cf. Eq. (15)), (B) from measurements of  $S$  (cf. Eq. (16)).

between these estimators and  $X(t)$  tends to zero, even for inaccurate initial conditions (Bastin and Dochain, 1990).

These estimators can now be used to perform a *cross-validation* of the parameter estimates  $\hat{k}_1$  and  $\hat{k}_2$  from the growth phase of two other experiments (E and F). The biomass estimate  $\hat{X}(t)$  is computed from the nitrogen and sugar measurements and compared to the actual values of  $X(t)$ . The quality of the cross-validation may be appreciated in Fig. 2.

### Mycelial Growth During the Biotransformation

We now intend to examine how the analysis above can be extended to describe the fungus growth during the production phase. We first observe that the biomass concentration is decreasing during vanillin production in all five experiments B, C, D, E, and F, with a decay rate which is much larger than the dilution rate  $D$  (see Fig. 3). This is inter-

preted as a significant biomass mortality probably due to a toxic effect of the phenolic compounds.

A new reaction must then be added to account for the mortality of the fungus:



where  $X_d$  is the dead biomass. The biomass dynamics will now be described by the following equations:

$$\frac{dX}{dt} = r_1 - r_2 - DX, \quad (18)$$

$$\frac{dX_d}{dt} = r_2 - DX_d, \quad (19)$$

where  $r_2$  denotes the fungal death rate.

By summing these two equations, we obtain an equation identical to Eq. (2):

$$\frac{dX_T}{dt} = r_1 - DX_T, \quad (20)$$

which describes the evolution of the total amount of produced biomass  $X_T = X + X_d$  during the biotransformation.

Following an argumentation similar as above the estimators  $\hat{X}_1(t)$  and  $\hat{X}_2(t)$  given by Eqs. (15) and (16) can be applied to estimate the total produced biomass  $X_T$  during the biotransformation. Such a computation has been performed for experiment C and is shown in Fig. 4 where we observe a large discrepancy between these two estimators: the biomass production predicted by the sugar consumption is much larger than the biomass production computed from nitrogen consumption. Indeed sugars are still consumed while consumption of ammonium has more or less stopped. It is therefore reasonable to assume that sugars are utilized not only for growth but also for the secondary metabolism. This assumption is introduced in the biotransformation model presented hereafter.

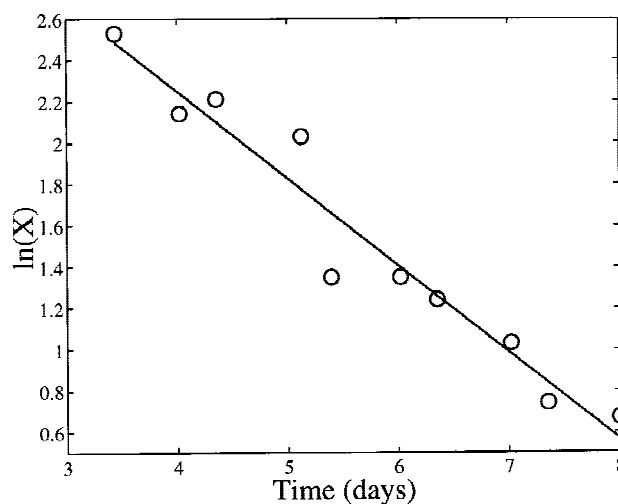


**Figure 3.** Logarithm of the biomass for experiment D during the biotransformation phase.

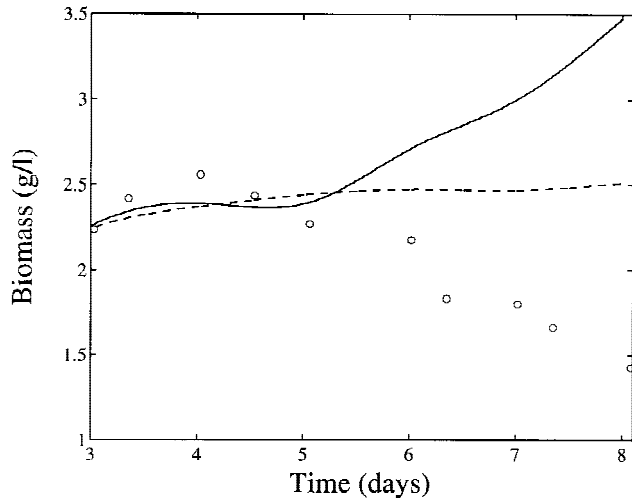
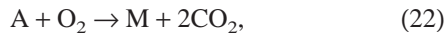


**Figure 4.** Estimation of the total produced biomass  $X_T$  during the biotransformation phase for experiment C from measurements of  $S$  (continuous line) (cf. Eq. (15)) and from measurements of  $N$  (dashed line) (cf. Eq. (16)).

### Biotransformation

It has been established (Falconnier et al., 1994; Lesage-Meessen et al., 1996) that the conversion of vanillic acid ( $A$ ) into vanillin ( $V$ ) by *P. cinnabarinus* usually proceeds along with two other competing reactions: an oxidation of vanillic acid into methoxyhydroquinone ( $M$ ) and a reduction of vanillin into vanillyl alcohol ( $L$ ). The reaction scheme is then as follows:



The first reaction includes sugar ( $S$ ) as a cofactor source (with a yield coefficient  $k_4$ ) in accordance with our previous observations.

The mass balances of vanillic acid, methoxyhydroquinone, and vanillyl alcohol are expressed by the following equations:

$$\frac{dA}{dt} = -r_3 - r_4 + DA_{\text{in}} - DA, \quad (24)$$

$$\frac{dV}{dt} = r_3 - r_5 - DV, \quad (25)$$

$$\frac{dM}{dt} = r_4 - DM, \quad (26)$$

$$\frac{dL}{dt} = r_5 - DL, \quad (27)$$

where  $r_3$ ,  $r_4$ , and  $r_5$  denote the reaction rates of vanillin, methoxyhydroquinone and vanillyl alcohol production respectively.  $A_{\text{in}}$  is the vanillic acid concentration in the feeding flow.

Moreover the sugar mass balance equation must be modified as:

$$\frac{dS}{dt} = -k_2 r_1 - k_4 r_3 - DS + DS_{\text{in}}. \quad (28)$$

### Estimation of $k_4$

In order to estimate the coefficient  $k_4$ , the reaction rates  $r_1$ ,  $r_3$  and  $r_5$  are eliminated between Eqs. (25), (27), (28), and (3):

$$\frac{d}{dt} \left[ \frac{k_2}{k_1} N + S + k_4(L + V) \right] = -D \left[ \frac{k_2}{k_1} (N - N_{\text{in}}) + S - S_{\text{in}} + k_4(L + V) \right]. \quad (29)$$

After integration of this equation and using the notation in Eq. (9), we obtain the following linear relationship:

$$\begin{aligned} & -\frac{k_2}{k_1} \phi[N(t) - N_{\text{in}}] + k_4 \phi[L(t) + V(t)] + \phi[S(t) - S_{\text{in}}] \\ & - \left( \frac{k_2}{k_1} (N_{\text{in}} - N(0)) + S(0) - S_{\text{in}} + k_4(L(0) + V(0)) \right) = 0. \end{aligned} \quad (30)$$

A linear regression will then provide an estimate of  $k_4$ , and of  $k_2/k_1$ . Using experiments B and C, the following parameter estimates are obtained:

$$\hat{k}_4 = 0.42 \text{ g mmol}^{-1}, \quad (31)$$

$$\widehat{k_2/k_1} = 1.1 \text{ g mmol}^{-1}. \quad (32)$$

The estimation of  $k_2/k_1$  is in a good agreement with the values of  $\hat{k}_1$  and  $\hat{k}_2$  (cf. Eq. (12)).

To validate Eq. (30), data of experiments E and F have been used to compute numerical approximations of  $\phi[N(t) - N_{\text{in}}]$  and  $\phi[S(t) - S_{\text{in}}]$  at the interpolation instants. Eq. (30), with the parameter values given by (31) and (32), then provides estimates of  $\phi[L(t) + V(t)]$  for these time instants. Figure 5 presents the comparison of these estimates with the numerical approximation of  $\phi[L(t) + V(t)]$  directly computed from the measurements of  $V$  and  $L$ .

### Global Mass Balance Model

On the basis of our previous developments, a general mass balance model valid for both the growth phase and the production phase can now be written by collecting Eqs. (3), (24)–(27), and (28) together. The model can be written under the compact matrix form (Bastin and Dochain, 1990);

$$\frac{d\xi}{dt} = Kr(\xi) - D\xi + D\xi_{\text{in}}, \quad (33)$$

with the following definitions:

$$\xi = \begin{pmatrix} X \\ X_d \\ S \\ N \\ A \\ V \\ M \\ L \end{pmatrix}, K = \begin{pmatrix} 1 & -1 & 0 & 0 & 0 \\ 0 & 1 & 0 & 0 & 0 \\ -k_2 & 0 & -k_4 & 0 & 0 \\ -k_1 & 0 & 0 & 0 & 0 \\ 0 & 0 & -1 & -1 & 0 \\ 0 & 0 & 1 & 0 & -1 \\ 0 & 0 & 0 & 1 & 0 \\ 0 & 0 & 0 & 0 & 1 \end{pmatrix}, \quad (34)$$

$$r = \begin{pmatrix} r_1 \\ r_2 \\ r_3 \\ r_4 \\ r_5 \end{pmatrix}, \xi_{in} = \begin{pmatrix} 0 \\ 0 \\ S_{in} \\ N_{in} \\ A_{in} \\ 0 \\ 0 \\ 0 \end{pmatrix}. \quad (35)$$

### Estimation of the Reaction Rates

The mass balance model of Eq. (33) can now be used to estimate the time evolution of the reaction rates from the data.

#### Estimation of $r_1$ and $r_2$

During the growth phase, we assume that the mortality may be neglected. The growth rate  $r_1$  can then be expressed as

$$r_1 = \left( DX + \frac{dX}{dt} \right), \quad (36)$$

or, from Eq. (5), as:

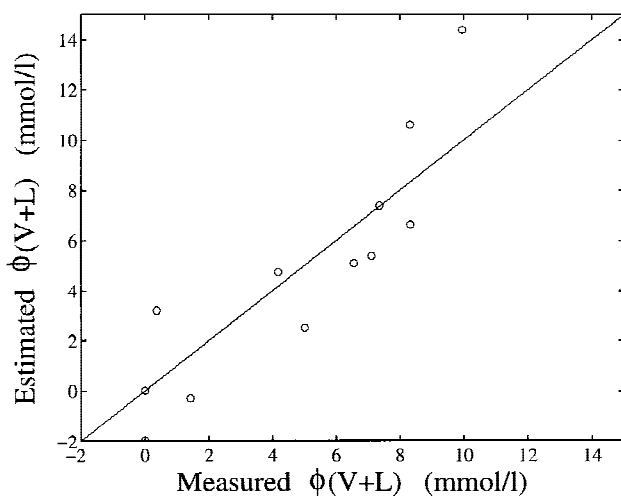


**Figure 5.** Cross-validation of Eq. (30) with experiments E and F. The figure presents a comparison of the predictions and of the direct measurements of the term  $\phi[L(t) + V(t)]$  from the available measurements of  $S$  and  $N$ .

$$r_1 = -\frac{1}{k_1} \left( DN - DN_{in} + \frac{dN}{dt} \right), \quad (37)$$

while the mortality rate  $r_2$  is set to zero. Eq. (36) will be preferred for the computation of  $r_1$  because expression Eq. (37) is based on the estimated parameters  $k_1$  and on nitrogen measurements that are less reliable.

During the production phase, as we have seen above, it is reasonable to assume that the growth phase is stopped since there is no significant consumption of nitrogen (see Fig. 4). The growth rate  $r_1$  is therefore set to zero. However, there is an important decay of the biomass, interpreted as a mortality rate  $r_2$  expressed as

$$r_2 = - \left( DX + \frac{dX}{dt} \right). \quad (38)$$

Finally the two situations may be summarized in single expressions which are valid for the two phases:

$$r_1 = \max \left( 0, \left( DX + \frac{dX}{dt} \right) \right), \quad (39)$$

$$r_2 = \max \left( 0, - \left( DX + \frac{dX}{dt} \right) \right). \quad (40)$$

#### Estimation of $r_3$ , $r_4$ and $r_5$

Eqs. (26) and (27) and the sum of Eqs. (25) and (27) lead to the following estimates of the reaction rates:

$$r_3 = \left( DV + \frac{dV}{dt} \right) - \left( DL + \frac{dL}{dt} \right), \quad (41)$$

$$r_4 = \left( DM + \frac{dM}{dt} \right), \quad (42)$$

$$r_5 = \left( DL + \frac{dL}{dt} \right). \quad (43)$$

The righthand side of these relations is used to compute estimates of the reaction rates. Cubic splines (MATLAB Toolbox) are used to interpolate and smooth the data (see Fig. 1) and are then differentiated numerically to compute approximations of the derivatives of the state variables. For instance, the first reaction rate is estimated as follows at interpolation instants  $t_j$

$$\hat{r}_1(t_j) = [DX_S(t_j) + \Delta X_S(t_j)], \quad (44)$$

where  $X_S(t_j)$  denotes the smoothing spline function of the biomass data and  $\Delta X_S(t_j)$  a numerical approximation of derivative at time  $t_j$ .

Similar expressions are derived for the other reaction rates. The result of these estimations is presented in Fig. 6.

### Kinetic Modeling

At this stage we obtained a mass balance model (Eq. (33)) that summarizes the main mass transformations inside the bioreactor. Such a mass balance model may be used for

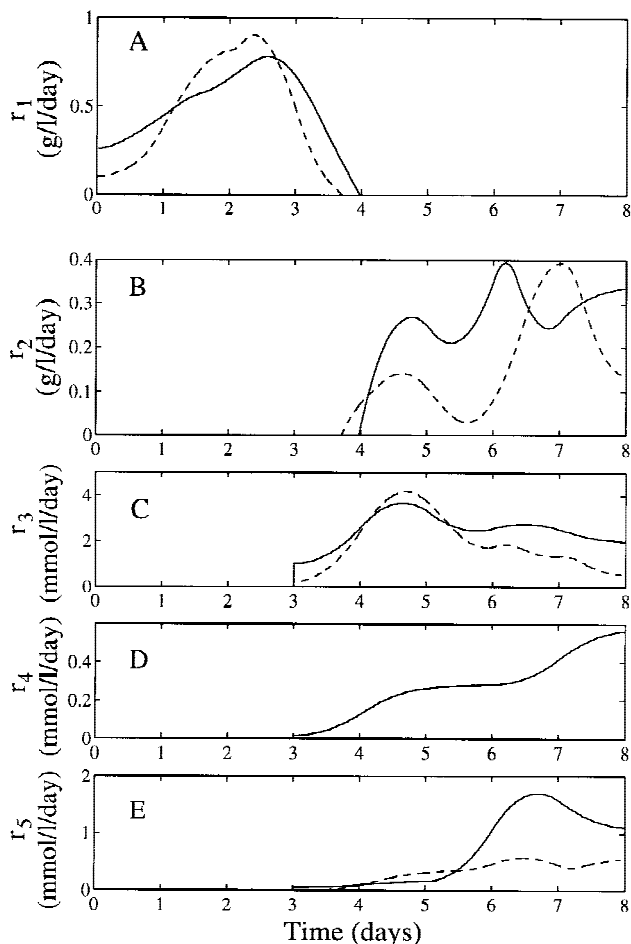


**Figure 6.** Estimation of the reaction rates for experiment B (dashed line) and C (continuous line) using Eqs. (39)–(43).

process monitoring or process control purpose without kinetic modeling being necessary (Bastin and Dochain, 1990).

But if a simulation model is required, then the modeling task is far from being completed: indeed an analytical expression of the reaction rates as a function of the process variables still needs to be determined.

In this section we propose an analytical expression for these five reaction rates. Currently, there does not exist any systematic approach to derive these reaction rates from a set of data. Moreover, we have to keep in mind that the choice of the analytical expressions of the  $r_i$  such that the model can simulate properly the data is generally not unique: several expressions for the reaction rates can lead to the same adequacy between the simulations and the experimental measurements. In this paper we restrict the choice of the analytical expressions to rational fractions of the components present in the bioreactor. We will therefore represent the effect of a substrate  $P$  necessary for the reaction by a Michaelis–Menten term  $P/(P + K_p)$  where  $K_p$  is the half-saturation constant. If  $P$  inhibits the reaction, we will choose an hyperbolic inhibition effect:  $K_i/(P + K_i)$ , with  $K_i$  the inhibition constant.

In order to select an appropriate expression for the kinet-

ics, we combine together three kinds of information that are now available: the prior knowledge available in the literature for other fungi, the experimental observations and the analysis of the reaction rates with respect to time, as they have been previously estimated (cf. Eqs. (39)–(43) and Fig. 6).

In order to avoid the problem of overfitting which may produce good results for the calibration but poor prediction capabilities of the model with new data, we try to find parsimonious mathematical expressions of the kinetics and to minimize the number of parameters.

### Modeling of the Growth Rate

Figure 7 shows that during the batch growth phase the biomass growth is strictly exponential. This indicates that the growth rate  $r_1$  is proportional to the biomass concentration. The substrates (carbon and ammonium) necessary for biomass growth are introduced in excess so that they are not limiting in the considered experiments.

The dissolved oxygen concentration in the medium is known to strongly influence the fungal growth (Suijdam et al., 1982). To account for this limiting effect of oxygen, we choose a Michaelis–Menten expression (Bajpai and Reuss, 1981).

The analysis of the estimation of  $r_1$  (see Fig. 6) points out that growth stops after addition of the phenolic compounds. To account for this inhibition effect, we adopt an hyperbolic inhibition function of the sum of the two main toxic compounds ( $V$  and  $A$ ). Finally, the growth kinetics is chosen as follows:

$$r_1 = r_{1m} \frac{O}{k_O + O} \frac{k_I}{k_I + V + A} X, \quad (45)$$

where  $k_O$  and  $k_I$  are the half-saturation constant with respect to oxygen and the inhibition constant with respect to the toxic phenolic compounds ( $V$  and  $A$ ), respectively.

The highest specific growth rate  $r_{1m}$  can be measured

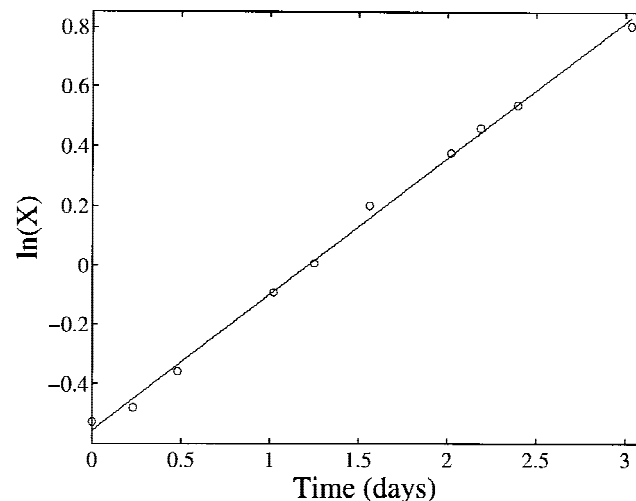


**Figure 7.** Logarithm of biomass for experiment C.



experimentally by growing the fungus in ideal conditions. We carried out a batch experiment where nutrients were maintained in excess and aeration was performed with pure oxygen to maintain the dissolved oxygen at saturation. In these conditions we measured a growth rate  $r_{1m} = 0.97 \text{ day}^{-1}$  during the exponential growth phase.

### Mortality of the Fungi

The death rate  $r_2$  increases significantly after addition of the phenolic compounds and we observe that the mortality rate is higher when the concentration of methoxyhydroquinone is high (see Fig. 1). We represent therefore the mortality as a Michaelis–Menten function of the methoxyhydroquinone. We take the same half-saturation constant  $k_1$  as the growth inhibition. We thus have the following expression for  $r_2$ :

$$r_2 = r_{2m} \frac{M}{k_1 + M} X. \quad (46)$$

The maximal death rate  $r_{2m}$  has been estimated in the biotransformation phase where the concentration of methoxyhydroquinone is high. Figure 3 shows that the biomass decreasing rate is exponential. The measured corresponding death rate is  $r_{2m} = 0.43 \text{ day}^{-1}$ .

### Reduction of Vanillic Acid into Vanillin

As it can be seen on Fig. 6, the vanillin production rate decreases along the biotransformation phase. We assume that the biotransformation is inhibited by the phenolic compounds, with  $k_1$  as inhibition constant.

Moreover oxygen seems to play a key role for vanillin production: when the level of oxygen is high, the vanillin production rate is very low while the methoxyhydroquinone production rate is high. It seems therefore that this reaction competes with methoxyhydroquinone production: oxygen triggers the reductive or the oxidative pathway.

We choose then the following expression:

$$r_3 = r_{3m} \frac{k_O}{k_O + O} \frac{k_1}{k_1 + V + A} \frac{A}{k_A + A} X, \quad (47)$$

where  $r_{3m}$  and  $k_A$  are the maximum vanillin production rate and the half-saturation constant with respect to  $A$ , respectively.

In order to minimize the number of different parameters in the model, the oxygen inhibition constant  $k_O$  in the production rate  $r_3$  is forced to be identical to the oxygen half-saturation constant in the growth rate  $r_1$ . The goal is to have a better conditioning of the parameter estimation problem that will be described hereafter. This simplification of the parameterization is the result of a preliminary step in the model development which is not described here for sake of brevity. We had first tried different values for  $k_O$  in  $r_1$  and  $r_3$ , but they were found to have close enough values to be aggregated in a single parameter. Obviously, there is not any biological motivation under this choice.

### Oxidation of Vanillic Acid into Methoxyhydroquinone

Consistently with the previous section, we choose the following relationship to express the methoxyhydroquinone production rate  $r_4$ :

$$r_4 = r_{4m} \frac{O}{k_O + O} \frac{V + A}{k_1 + V + A} \frac{A}{k_A + A} X, \quad (48)$$

where  $r_{4m}$  is the maximum production rate of methoxyhydroquinone  $r_4$ .

### Reduction of Vanillin into Vanillyl Alcohol

We assume that this reaction depends only on the vanillin concentration:

$$r_5 = r_{5m} \frac{V}{k_V + V} X, \quad (49)$$

where  $k_V$  is the half-saturation constant with respect to  $V$  and  $r_{5m}$  the maximum production rate of vanillyl alcohol.

### Calibration of the Model

The yield coefficients associated with the general mass balance model in Eq. (33) have been identified while the mass balance model was worked out. The other parameters, related to the expression of the kinetics are of two types: the parameters that can be estimated directly using some part of experiments (maximum growth rate, maximum death rate, . . .), and the parameters which will be estimated globally by a minimization procedure. For the latter the MATLAB function `fmins` (Nelder–Mead simplex search (Nelder and Mead, 1965)) has been used to obtain the value of the parameters which minimize the prediction error  $J$ :

$$J = \sum_i \left( \frac{\xi_i(t_j) - \hat{\xi}_i(t_j)}{\bar{\xi}_i} \right)^2, \quad (50)$$

where  $\hat{\xi}_i(t_j)$  is the simulated  $i$ th variable at the measurement instant  $t_j$  and  $\bar{\xi}_i$  is a normalization constant corresponding to the average value of the  $\xi_i$  for all available measurements.

The parameters values have been computed using together experiments A, B, C and D. Table 2 summarizes the obtained parameter values.

### Sensitivity Analysis

In order to assess how the model predictions may be sensitive to errors in the parameter estimates, a sensitivity analysis has been performed as follows.

The parameter values of Table II are taken as nominal values. The solutions of the model equations are then computed with relative parameter errors ranging from  $-50\%$  to  $+50\%$  of the nominal values. The final concentrations of biomass  $X$ , vanillin  $V$  and methoxyhydroquinone  $M$  are then

**Table II.** Kinetic parameters for the simulation model.

Parameter	Meaning	Unit	Value	Estimation <sup>a</sup>
$r_{1m}$	Max. growth rate	day <sup>-1</sup>	0.97	D
$r_{2m}$	Max. death rate	day <sup>-1</sup>	0.43	D
$r_{3m}$	Max. bioconversion rate of $V$	mmol (g day) <sup>-1</sup>	11.9	D
$r_{4m}$	Max. bioconversion rate of $H$	mmol (g day) <sup>-1</sup>	4.81	D
$r_{5m}$	Max. bioconversion rate of $L$	mmol (g day) <sup>-1</sup>	0.31	G
$k_O$	Inhibition/half-saturation constant for $O_2$	% saturation	10.67	G
$k_I$	Inhibition/half-saturation constant for $V + A$	mmol L <sup>-1</sup>	1.2	G
$k_A$	Half-saturation constant for $A$	mmol L <sup>-1</sup>	0.73	G
$k_V$	Half-saturation constant for $V$	mmol L <sup>-1</sup>	6.25	G

<sup>a</sup>D, directly estimated; G, globally estimated by minimizing the prediction error.

compared to the nominal concentrations. The results are represented in Fig. 8.

The two most critical parameters are by far  $r_{1m}$  (the maximal biomass growth rate) and  $k_O$  (which is the oxygen inhibition constant in  $r_3$  and the half-saturation constant in  $r_1$  and  $r_4$ ). This is easily explained as follows.

The parameter  $r_{1m}$  determines the amount of biomass produced during the growth phase. The subsequent bio-transformation is then proportional to this biomass amount. The parameter  $k_O$  not only has an influence on the biomass growth but it determines also the triggering between oxidative and reduction pathways. In fact, the sensitivity of the

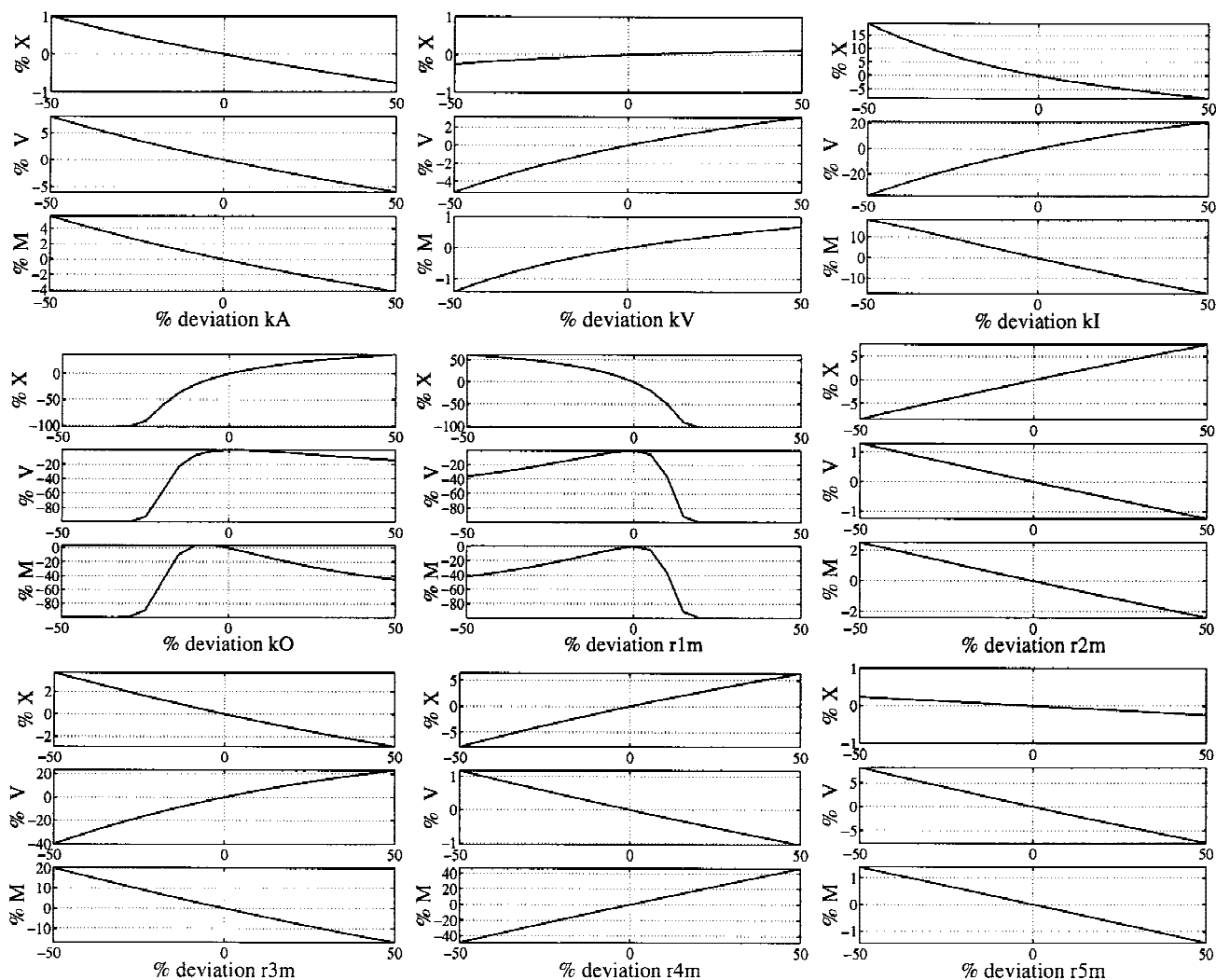


**Figure 8.** Sensitivity analysis for the kinetic parameters of the model. The changes in the final value of the biomass, vanillin, and methoxyhydroquinone concentrations are represented with respect to the deviation of the nominal value of the considered parameter.

model to  $k_O$  reflects the sensitivity of the process to the oxygen concentration. Indeed, the activation and inhibition terms related to oxygen may be written respectively as

$$\frac{O/k_O}{1 + O/k_O} \text{ and } \frac{1}{1 + O/k_O}.$$

It can be seen that the effect of a variation of the parameter  $k_O$  must be equivalent to the effect of an inverse variation of the oxygen concentration with the same magnitude.

To a lesser extent, the biomass concentration  $X$  is also

sensitive to  $k_1$  while the vanillin  $V$  and methoxyhydroquinone  $M$  concentrations are sensitive to  $k_1$ ,  $r_{3m}$ , and  $r_{4m}$ . Finally, the model predictions are almost insensitive to the other parameters  $k_A$ ,  $k_V$ ,  $r_{2m}$ , and  $r_{5m}$ .

### Model Validation

Figure 9 presents the simulation results obtained with experiments B, C, and D. The simulation is very close to the

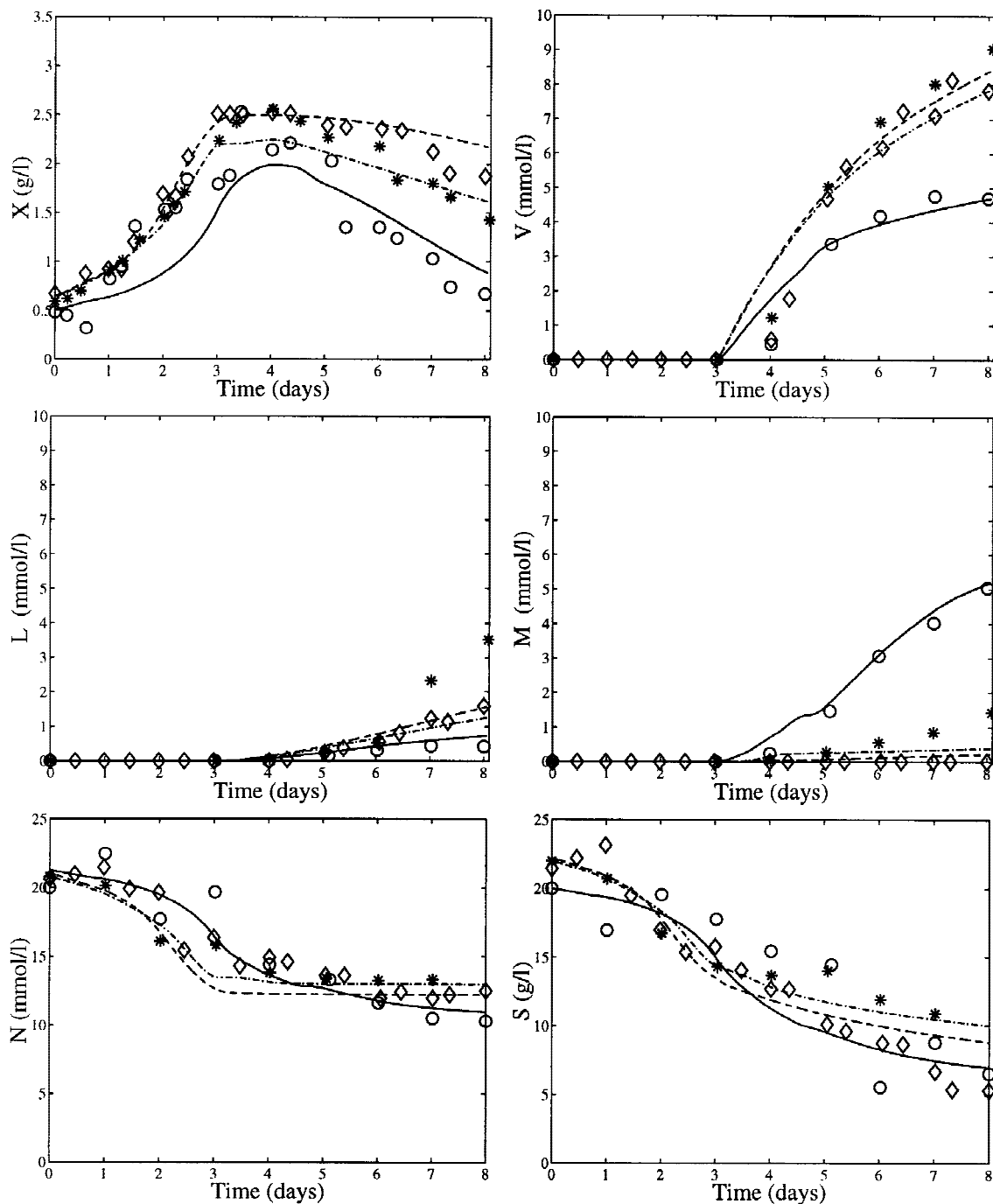


Figure 9. Simulation results for experiment B (data,  $\diamond$ ; simulations, - -), C (data,  $*$ ; simulations, - -), and D (data,  $o$ ; simulations, —).

actual data. A defect of the model should nevertheless be mentioned. A delay for the vanillin production is observed which is not reproduced in the simulations: in the experiments vanillin appears almost 1 day after the addition of the vanillic acid. This latent phase is probably due to the time necessary for the intracellular uptake of the phenolic compounds and their release in the medium. The lag induced by these transport phenomenon is not taken into account in the model. Nevertheless this delay does not affect the accuracy

of the predicted final amount of vanillin which is quite close to the quantity which is actually measured.

The model predictions are then compared with experiments E and F which have not been used for the calibration of the model. The results of this cross-validation are good, as can be seen in Figure 10. The phenolic compounds, the sugars and the nitrogen are accurately predicted.

The biomass prediction for experiment E is lower than the actual values: in this experiment biomass continues to

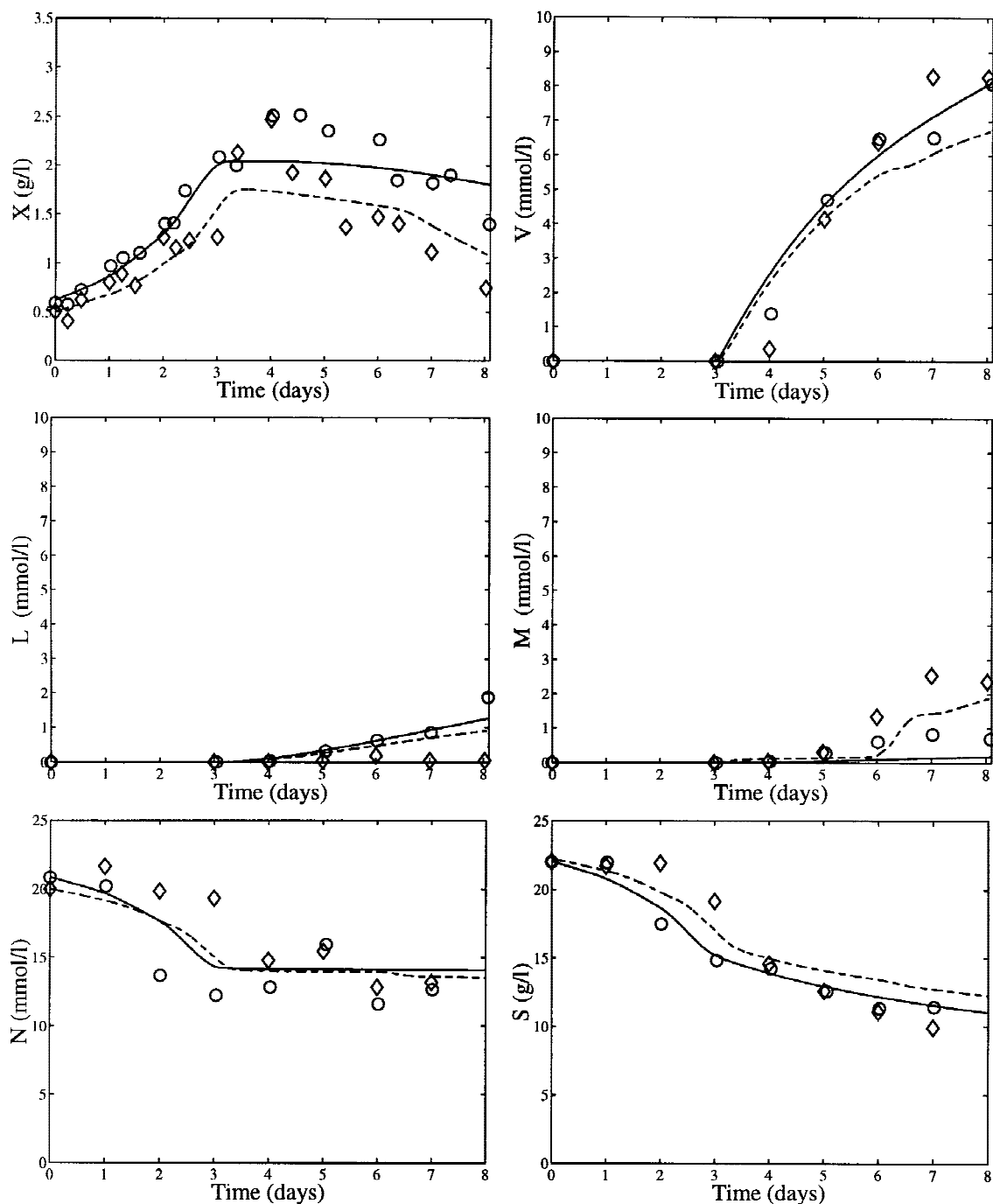


Figure 10. Cross validation results for experiment E (data, o; simulations, —) and F (data,  $\diamond$ ; simulations, - -).

grow for 36 h despite the addition of the precursor. However, the error on biomass does not affect the prediction of the other variables. In particular, the final amount of produced vanillin is accurately predicted.

## CONCLUSION

This paper is an illustration of the general modelling approach used to identify a model from a series of experiments (Bastin et al., 1997). The important point in this approach is that we separate clearly the identification of the structure of the model (with mass balance equations) from the identification of the analytical expression of the kinetics.

It is emphasized that the second task can not be performed if the first one has not been carried out properly, i.e. if the structure of the model is not correct. Anyway the kinetic modeling is still a difficult task for bioprocesses, where a succession of choices must be done for which systematic methodologies are still lacking. Therefore it is important that this step be validated using cross validation with data which were not used to identify the parameters. To increase the prediction capabilities of the model, the number of parameters must be minimized to avoid overfitting that generally leads to a bad cross-validation of the model. This is the reason why in our model we have tried to limit the number of parameters (3 yield coefficients and 9 kinetic parameters).

The proposed model turns out to predict acceptably the evolution of the variables during the growth and the bio-transformation phases. In spite of delays that are not involved, the final amount of produced vanillin is accurately predicted. Moreover, the model accounts for the high sensitivity of the process to the concentration of dissolved oxygen which seems critical in triggering the reductive or the oxidative pathway.

Associated with the model, we derived also estimators for the biomass and for the sum of vanillin and vanillyl alcohol concentrations. These estimators, together with the estimators of the reaction rates can be used in on-line monitoring procedures and optimal control (Bastin and Dochain, 1990; Bastin and Van Impe, 1995) of the vanillin production process.

## NOMENCLATURE

$A$	vanillic acid concentration (mmol L <sup>-1</sup> )
$A_{in}$	feeding vanillic acid concentration (mmol L <sup>-1</sup> )
$D$	dilution rate (day <sup>-1</sup> )
$k_1$	yield coefficient for nitrogen (mmol g <sup>-1</sup> )
$k_2$	yield coefficient for sugar (growth) (mmol g <sup>-1</sup> )
$k_4$	yield coefficient for sugar (biotransformation) (mmol g <sup>-1</sup> )
$k_A$	vanillic acid half-saturation constant (mmol L <sup>-1</sup> )
$k_I$	inhibition/half-saturation constant for the phenolic compounds (mmol L <sup>-1</sup> )
$k_O$	oxygen inhibition/half-saturation constant (%)
$k_V$	vanillin half-saturation constant (mmol L <sup>-1</sup> )
$L$	vanillyl alcohol concentration (mmol L <sup>-1</sup> )
$M$	methoxyhydroquinone concentration (mmol L <sup>-1</sup> )
$N$	nitrogen concentration (mmol L <sup>-1</sup> )

$N_{in}$	feeding nitrogen concentration (mmol L <sup>-1</sup> )
$O$	dissolved oxygen concentration (%)
$r_1$	growth rate (day <sup>-1</sup> )
$r_2$	death rate (day <sup>-1</sup> )
$r_3$	vanillin bioconversion rate (mmol (g day) <sup>-1</sup> )
$r_4$	methoxyhydroquinone bioconversion rate (mmol (g day) <sup>-1</sup> )
$r_5$	vanillyl alcohol bioconversion rate (mmol (g day) <sup>-1</sup> )
$r_{1m}$	max. growth rate (day <sup>-1</sup> )
$r_{2m}$	max. death rate (day <sup>-1</sup> )
$r_{3m}$	max. vanillin bioconversion rate (mmol (g day) <sup>-1</sup> )
$r_{4m}$	max. methoxyhydroquinone bioconversion rate (mmol (g day) <sup>-1</sup> )
$r_{5m}$	Max. vanillyl alcohol bioconversion rate (mmol (g day) <sup>-1</sup> )
$S$	sugar concentration (g L <sup>-1</sup> )
$S_{in}$	feeding sugar concentration (g L <sup>-1</sup> )
$V$	vanillin concentration (mmol L <sup>-1</sup> )
$X$	living mycelial biomass (g L <sup>-1</sup> )
$X_d$	dead mycelial biomass (g L <sup>-1</sup> )
$x_T$	total mycelial biomass (g L <sup>-1</sup> )

We thank the anonymous reviewers who have provided very interesting suggestions to improve the paper. This paper presents research results of the Belgian Program on the Interuniversity Poles of Attraction initiated by the Belgian State, Prime Minister's Office, Science Policy Programming. The scientific responsibility rests with its authors. This work was also partially supported by the European Research Programme ERB-FAIR-CT96-1099, "Design and scale-up of a bioprocess for the production of natural vanillin from agricultural by-products". C. S. thanks the Institut National de la Recherche Agronomique, the Conseil Régional Provence-Alpes-Côte d'Azur, and Orangina CECO for a Ph.D. scholarship.

## References

- Aynsley M, Ward A, Wright A. 1990. A mathematical model for the growth of mycelial fungi in submerged culture. *Biotechnol Bioeng* 35:820-830.
- Bajpai R, Reuss M. 1981. Evaluation of feeding strategies in carbon-regulated secondary metabolite production through mathematical modeling. *Biotechnol Bioeng* 23:717-738.
- Bastin G, Bernard O, Chen L, Chotteau V. 1997. Identification of mathematical models for bioprocess control. Proc. eleventh Forum Appl Biotechnol, 11th, Gent, September 1997, 2:1559-1572.
- Bastin G, Dochain D. 1990. On-line estimation and adaptive control of bioreactors. Amsterdam: Elsevier Science.
- Bastin G, Levine J. 1992. On state accessibility in reaction systems. *IEEE Trans Autom Control* 38:83-88.
- Bastin G, Van Impe J. 1995. Nonlinear and adaptive control in biotechnology: A tutorial. *Eur J Control* 1:1-37.
- Falconnier B, Lapierre C, Lesage-Meessen L, Yonnet G, Brunerie P, Colonna-Ceccaldi B, Corrieu G, Asther M. 1994. Vanillin as a product of ferulic acid biotransformation by the white-rot fungus *Pycnoporus cinnabarinus* I-937: Identification of metabolic pathways. *J Biotechnol* 37:123-132.
- Gross-Falconnier B. 1994. Production de molécules aromatisantes par des Basidiomycètes: étude d'une biosynthèse et d'une bioconversion réalisées par *Pycnoporus cinnabarinus*. PhD thesis, University Paris Sud, Orsay, F.
- Lesage-Meessen L, Delattre M, Haon M, Thibault J, Colonna-Ceccaldi B, Brunerie P, Asther M. 1996. A two-step bioconversion process for vanillin production from ferulic acid combining *Aspergillus niger* and *Pycnoporus cinnabarinus*. *J Biotechnol* 50:107-113.
- Lesage-Meessen L, Haon M, Delattre M, Thibault J, Colonna-Ceccaldi B, Asther M. 1997. An attempt to channel the transformation of vanillic acid into vanillin by controlling methoxyhydroquinone formation in

- Pycnoporus cinnabarinus* with cellobiose. Appl Microbiol Biotechnol 47:393–397.
- Nelder J, Mead R. 1965. A simplex method for function minimization. Computer J 7:308–313.
- Nestaas E, Wang D. 1983. Computer control of the penicillin fermentation using the filtration probe in conjunction with a structured process model. Biotechnol Bioeng 25:781–796.
- Paul G, Thomas C. 1996. A structured model for hyphal differentiation and penicillin production using *Penicillium chrysogenum*. Biotechnol Bioeng 51:558–572.
- Suijdam JV, Hols H, Kossen N. 1982. Unstructured model for growth of mycelial pellets in submerged cultures. Biotechnol Bioeng 24:177–191.
- Torres N. 1994. Modeling approach to control of carbohydrate metabolism during citric acid accumulation by *Aspergillus niger*: I. Model definition and stability of the steady state. Biotechnol Bioeng 44:104–111.